Proceedings World Geothermal Congress 2015
Melbourne, Australia, 19-25 April 2015

Geochemical Modeling of Acidic Geothermal Fluids using SOLVEQ and CHIM-xpt

Emily Ann A. Bartolo[1] and Mark H. Reed[2]

[1]Energy Development Corporation Ortigas Centre, Pasig City Philippines

[2]Department of Geological Sciences, University of Oregon, Eugene, OR, 97403

Email: bartolo.ea@energy.com.ph

Keywords: *SOLVEQ-xpt, CHIM-xpt, deep seated acidity,* SO_2/H_2SO_4*, excess iron, water-rock interaction*

ABSTRACT

Drilling and field development in geothermal systems can be hindered by acidic fluids. It is essential to understand the source and mechanism of acidity in the early stages of exploration in order to formulate a suitable development strategy.

The objective of this study is to understand the origin of fluid acidity in an andesitic geothermal system of Mt. Labo, Philippines. This is done by computer modeling with the aid of geochemical software SOLVEQ-xpt and CHIM-xpt. Chemical composition of acidic fluids discharged from exploration wells in the postulated upflow zone was used as starting point. The core of the software is a geochemical speciation algorithm for solving mass balance and mass action equations at various temperatures and pressures by Newton-Raphson iterations (Reed, 1998). The analyses of gas and liquid samples from the well discharge are combined to reconstruct the reservoir fluid conditions using SOLVEQ. CHIM is used to model the reaction of the reservoir fluid with either the host rock or well casing material.

The chemical analyses data of gas and liquid samples obtained from the surface were combined and recalculated to reservoir fluid conditions at 276°C and 6.04 MPa pressure. The resulting fluid is modeled for adiabatic boiling by depressurization to 100°C and 0.1MPa using CHIM. Results of boiling calculation show: 1) significant concentration of aqueous sulfate, bisulfate and sulfide, inferred to be from the disproportionation of magmatic SO_2 forming H_2S and H_2SO_4; and 2) formation of significant amounts of pyrite due to the high iron concentration of the fluid. To determine whether high iron concentration originates from water-rock interaction or is caused by casing corrosion, an andesite type rock was reacted with a primary acidic fluid. The result show maximum aqueous Fe concentrations far smaller than analysed in the actual well fluid. In contrast, the computed reaction of the primary acidic fluid with the wellbore steel casing yielded high Fe concentrations. This result is consistent with the observed casing corrosion in the well.

Modeling results also show that the reservoir fluid pH increases after reaction with the host rock. The water-rock ratio in the reservoir was approximated by comparing the acid alterations formed in the model to the actual acid mineral alterations identified from the drill cuttings. The alteration minerals produced from the model such as alunite, pyrophyllite, quartz, pyrite, anhydrite and chlorite match the observed mineral alteration of rock cuttings from the wells at depths where temperature is greater than 270°C. The model shows that at the most acidic condition, the fluid has pH < 3.5 and temperature of 276°C. At this condition the acid alteration minerals were in equilibrium with the acidic reservoir fluids. Furthermore, the high iron concentration in the well discharge is attributed to casing corrosion. This is because iron-bearing alteration minerals such as pyrite, and iron silicate mineral such as chlorite limits the iron concentration from rock reaction to much lower values. In conclusion, the acidity of the fluid is deep seated in the postulated upflow. The fluid may be neutralized as it interacts with the host rocks while flowing towards the outflow region of the system.

1. INTRODUCTION

Mt. Labo

The development of andesitic geothermal systems can be hindered by acidic fluids. Mt. Labo is an example of this type of system. It is located in the island of Luzon of the Philippine archipelago (Figure 1) and is part of the 200 km long Bicol volcanic chain of stratovolcanoes. Arc volcanism in the Bicol region is related to the westward subduction of the Philippine Sea Plate along the Philippine Trench in the east which progress at an average rate of 8 cm/yr. (Aurelio, 2000). The regional basement rock consists of Pre-Cretaceous metamorphic and Cretaceous ultramafics which is uncomformably overlain by Tertiary sediments and volcanic rocks (JICA, 1999).

Mt. Labo is an inactive andesitic stratovolcano. Two rock formations were mapped: the Pleistocene to recent Labo volcanics (Lbv) and the Pliocene Susung Dalaga Formation (Sdf). The Lbv is a collective name for the Pleistocene volcanic rocks that directly overlies the Sdf and is widely distributed in the field. It consists mainly of andesite and some dacite blocks. The Sdf refers to the volcanics exposed in the west of Mt. Labo that consists of Early Pliocene andesitic to dacitic lava flows. In the subsurface, this formation is intermixed with modest amounts of carbonaceous with varying calcareous marine sediments (Delfin, et al, 1995).

Some of the geothermal wells drilled on the flanks of Mt. Labo volcano encountered acidic Cl-SO_4 type of waters with pH = 3, measured at 25°C. Discussions were made to identify if the source of acidity is shallow or deep. A shallow source was hypothesized as coming from the oxidation of H_2S at shallow levels producing H_2SO_4 that percolate down via permeable structures. Deep seated acidity it thought to come from the disproportionation of magmatic SO_2, which come into contact with deep aquifer fluid producing H_2SO_4 and H_2S at depth. The objective of this paper is to apply SOLVEQ-xpt and CHIM-xpt to understand the origins of fluid acidity in Mt. Labo, using the water and gas discharge chemical compositions of wells. Computer model can aid intuition building about the nature of the system when results are compared to real counterparts**.**

SOLVEQ-xpt and CHIM-xpt

The core of the software is a geochemical speciation algorithm for solving mass balance and mass action equations at various temperatures and pressures by Newton-Raphson iterations. Mass balance equations account for the distribution of thermodynamic components among gases, minerals and aqueous species. Mass action equations take into account the stabilities of complexes, ion pairs and redox species in the aqueous phase as well as the non-ideality of the salt solution, solid solutions and some gas phase species (Reed, 1998). The set of simultaneous equations is solved repeatedly with incremental changes in temperature, pressure, enthalpy or composition between steps by applying a Newton-Raphson method and using the SOLTHERM database (Reed et al, 2010), which contains all the relevant thermodynamic data.

The results of the simulations are presented in stacked graphs with a common x-axis, and different y-axes that show the minerals that formed, gas phase components (in Log mol/kg of solution) and the liquid phase components (in log total molality).

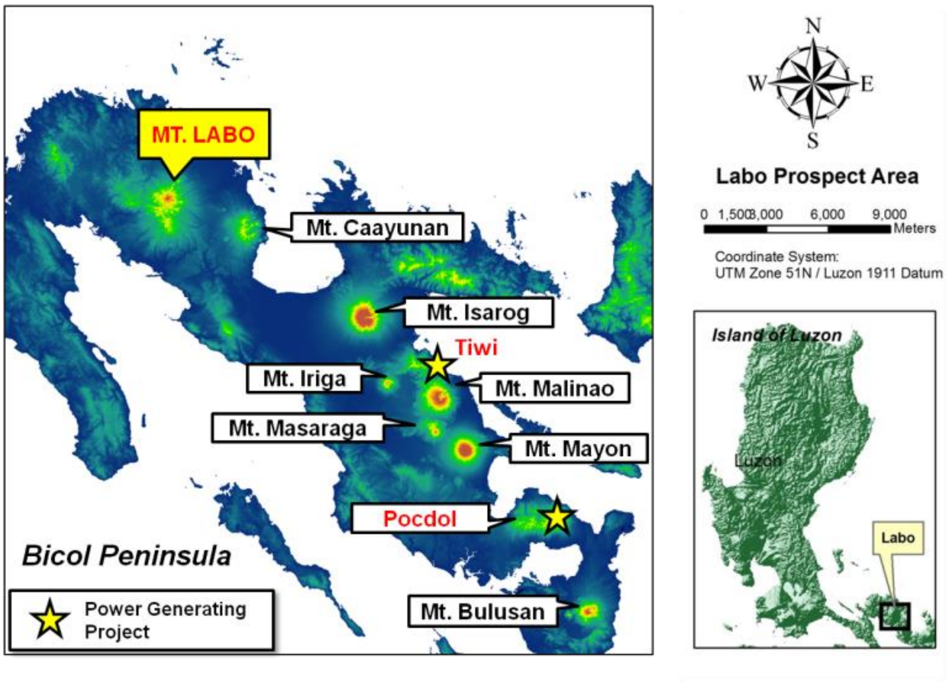

Figure 1: Location map of Mt. Labo Geothermal System in the island of Luzon, Philippines

2. WATER COMPOSITION AND BOILING

Using the laboratory analysis of the well discharge, the water and gas components were combined and computed to reservoir conditions. The lack of Al in the analysis was compensated by fixing the aluminum concentration with a certain Al alteration mineral that is known or supposed to be in the alteration assemblage at depth, the “FixAl” method discussed in detail by Pang and Reed (1998).The “FixAl” option is done in SOLVEQ by forcing the recombined liquid and gas components to be in equilibrium with a certain Al-bearing mineral in the reservoir. Selection of the Al-bearing mineral based on the numerical experiments carried out in this study show that in many slightly acidic waters, muscovite or kaolinite are suitable choices. Muscovite was selected as the Al-bearing mineral that fixes the concentration of aluminum in the well waters reported here.

The combined water and gas analyses (Table 1) are used as the starting fluid compositions for calculations presented in this report. These are fluids derived from Well #5, and Well #7 in Mt. Labo geothermal system. Liquid A is a modification of Well #5 fluids and is described in detail in the following sections. These two wells were selected to represent and understand the nature of the discharged fluids. Well #5 fluids is acidic with pH = 3.06 measured at 25 °C. The well was drilled at the flanks of the volcano targeting the postulated geothermal upflow. Well #7 fluids is neutral with pH = 7.49 at 25 °C. The well is drilled towards the outflow of geothermal system. The location of these wells is shown in Figure 4. The concentrations in Table 1 are expressed in total molality in the aqueous phase and the standard set of thermodynamic components is listed in the left-most column. The negative value of component SO_4^{2-} describes the composition of reduced waters, as discussed in detail by Reed (1992).

2.1 Boiling of the acidic well fluid

Well #5 fluids is computed to reservoir condition using SOLVEQ-XPT at temperature of 276°C and pressure of 6.04 MPa while Well #7 fluids are at 262°C and pressure of 4.85 MPa. The reservoir temperatures are based on quartz geothermometer calculation. Boiling of fluid from each well is modeled using CHIM-XPT to simulate the condition of the fluids as it ascends up the well. In both wells it is assumed that boiling of the fluid happens as the liquid rises inside the well. The subsequent change in temperature and pressure during boiling causes the formation of minerals which precipitate from the fluid as it ascends. Both gas and liquid phases are assumed to stay in contact throughout the ascent and the resulting minerals are continuously removed from the system. Quartz, cristobalite and chalcedony are not allowed to precipitate because their formation kinetics is slow. The rest of the minerals are allowed to form when thermodynamic supersaturation is reached. Boiling is also assumed to be isenthalpic i.e., heat is neither added nor removed between the surroundings and the boiling fluids. These assumptions are similar to that of Reed (1992).

The starting pH of Well #5 fluids at 276°C is 5.42. During boiling, the pH decreased in the first equilibration step of boiling accompanied by formation of pyrite (FeS_2) as shown in Figure 2. The decline in pH during the first boiling equilibration step can be attributed to an excess in Fe^{2+} in the starting water composition which drives Reaction 1 (below) towards the right. The starting water composition of Well #5 contains 157 ppm Fe^{2+}. There are two possible sources of the excess iron from this well: 1) from corrosion of wellbore casing and 2) from the host rock. How much of iron came from which source was quantified in Section 3.

As the fluids in Well #5 continue to boil and pyrite is fractionated, the pH continued its decreasing trend. The high SO_4^{2-} concentration of fluid from Well #5 (Table 1) is a result of a relatively oxidized aqueous phase. This is in contrast to the more reduced state of fluids in Well #7. The oxidized and acidic conditions apparently resulted from input of sulfuric acid that yield high concentration of $HSO_4^-{}_{aq}$ in the starting fluid compared to HCl_{aq} (0.2569E-04 m). The concentrations of $HSO_4^-{}_{aq}$ and HCl_{aq} remain elevated at high temperatures because these acids are more strongly associated at high temperatures than at lower temperatures. Decreasing temperatures brought about by boiling drives the dissociation of HSO_4^- and HCl (Equilibria 2 and 3, respectively). This is supported by the decreasing HSO_4^- and increasing SO_4^{2-} concentrations during boiling (Figure 2). The supply of H^+ therefore increases and exceeds the removal of H^+ by CO_2 degassing in Reaction 4.

$$2\mathrm{HS}^{-}_{,aq} + \mathrm{Fe}^{2+} \leftrightarrow \mathrm{FeS}_2,_{s} + 2\mathrm{H}^{+}_{aq} \qquad (1)$$

$$\mathrm{HSO}^{-}_{4,aq} \leftrightarrow \mathrm{H}^{+}_{aq} + \mathrm{SO}^{2-}_{4,aq} \qquad (2)$$

$$\mathrm{HCl} \leftrightarrow \mathrm{H}^{+}_{aq} + \mathrm{Cl}^{-}_{\backslash,aq} \qquad (3)$$

$$\mathrm{HCO}^{3-}_{aq} + \mathrm{H}^{+}_{aq} \leftrightarrow \mathrm{H_2O}_{aq,g} + \mathrm{CO}_{2(g)} \qquad (4)$$

Table 1 Starting water compositions

```
Aqueous Phase Total Molality

Species            W#5(pH 3.06, 25C)     W#7 (pH 7.49, 25C)          Liquid A

    H+             0.187                  0.583                      0.251
    Cl-            0.111                  0.889 E-01                 0.110
    SO4--          0.143 E-01            -0.332 E-02                 0.431 E-01
    HCO3-          0.182                  0.581                      0.180
    HS-            0.558 E-02             0.134 E-01                 0.554 E-02
    SiO2(aq)       0.102 E-01             0.518 E-02                 0.757 E-02
    Ca++           0.332 E-04             0.299 E-02                 0.330 E-04
    Mg++           0.527 E-02             0.219 E-05                 0.523 E-02
    Fe++           0.287 E-02             0.117 E-05                 0.722 E-20
    K+             0.904 E-02             0.619 E-02                 0.898 E-02
    Na+            0.111                  0.774 E-01                 0.110
    Mn++           0.996 E-03                                        0.722 E-21
    F-             0.590 E-04             0.127 E-03                 0.586 E-04
    NH4+           0.192 E-02             0.457 E-02                 0.191 E-02
    H3BO3          0.216 E-02             0.251 E-02                 0.214 E-02
    Al+++          0.173 E-05             0.510 E-05                 0.722 E-21
    Zn++                                                             0.722 E-22
    Cu+                                                              0.722 E-22
    Ni++                                                             0.722 E-22
    pH(T)          5.42 (276)             5.01 (262)                 2.0 (276)
```

2.2 Boiling of the neutral well fluid

The decreasing pH trend observed in boiling Well#5 is in contrast to the boiling simulation of Well #7. The reservoir water of Well #7 has a pH 5.01 at 262 °C. As the fluid ascends and boils, the pH increases to 6.64 at 101 °C as shown in Figure 2. The increase is largely driven by the escape of CO_2 to the gas phase as in Reaction 4. Although the dissociation of HSO_4^- during boiling also occur in Well #7, starting concentration of HSO_4^- is considerably lower in Well #7 (0.22530E-09Molal) than in Well #5 (0.9213 E-02 Molal), hence the liberated H^+ is lower and does not exceed the H^+ removal by CO_2 degassing.

The scale minerals formed in the Well #7 boiling run are dominated by initial formation of calcite at high temperature and abundant amorphous silica with trace pyrite at T < 150 °C. The computed trace amounts of Ca-Mg silicates (Figure 2) would not precipitate rapidly enough to form in the actual setting, but their components may appear as trace contamination of the abundant scale such as the amorphous silica.

2.3 Possible sources of acidity

The simulations show that the decrease in pH with boiling in Well #5 is driven by the dissociation of HSO_4^- (Reaction 2) with decreasing temperatures. This is proven by the increasing SO_4^{2-} and decreasing HSO_4^- concentrations in the boiling calculations plotted in Figure 2.

The initially large HSO_4^- concentration in Well #5 is likely sustained by H_2SO_4 from magmatic volatiles such as SO_2 which is scrubbed by hydrolysis involving disproportionation reactions as in Reactions 5 and 6. These reactions shift strongly to the right with cooling below 400 °C e.g., by Symonds et al. (2001). Acidic systems can also be sustained by atmospheric oxidation of condensed H_2S which also produces H_2SO_4 that percolates down through permeable structures; however, such acidic zones are shallow. Once the acid waters move away from the SO_2 supply, the reaction of the waters with the wall rocks neutralizes the acid and the boiling behavior shifts to the increasing pH-type as in simulations of Reed (1992).

These conclusions about acidity are consistent with the conceptual model of Mt. Labo geothermal system where Well #5 (Figure 4), drilled towards the upflow, discharged acidic fluids (pH 3.06, 25C) in contrast to Well # 7, drilled in the outflow zone discharged neutral fluids (pH 7.49, 25C). Fluids of Well #7, likely underwent sufficient water-rock reaction that neutralized the acid. It is thus expected that the geothermal environment evolves from an early acidic system to neutral-pH system as the influx of magmatic volatiles wanes over time.

$$4SO_{2,g} + 4H_2O,_{aq} \leftrightarrow H_2S,_g + 3H_2SO_{4,aq} \qquad (5)$$

$$3SO_{2,g} + 2H_2O,_{aq} \leftrightarrow S,_{s,l} + 2H_2SO_{4,aq} \qquad (6)$$

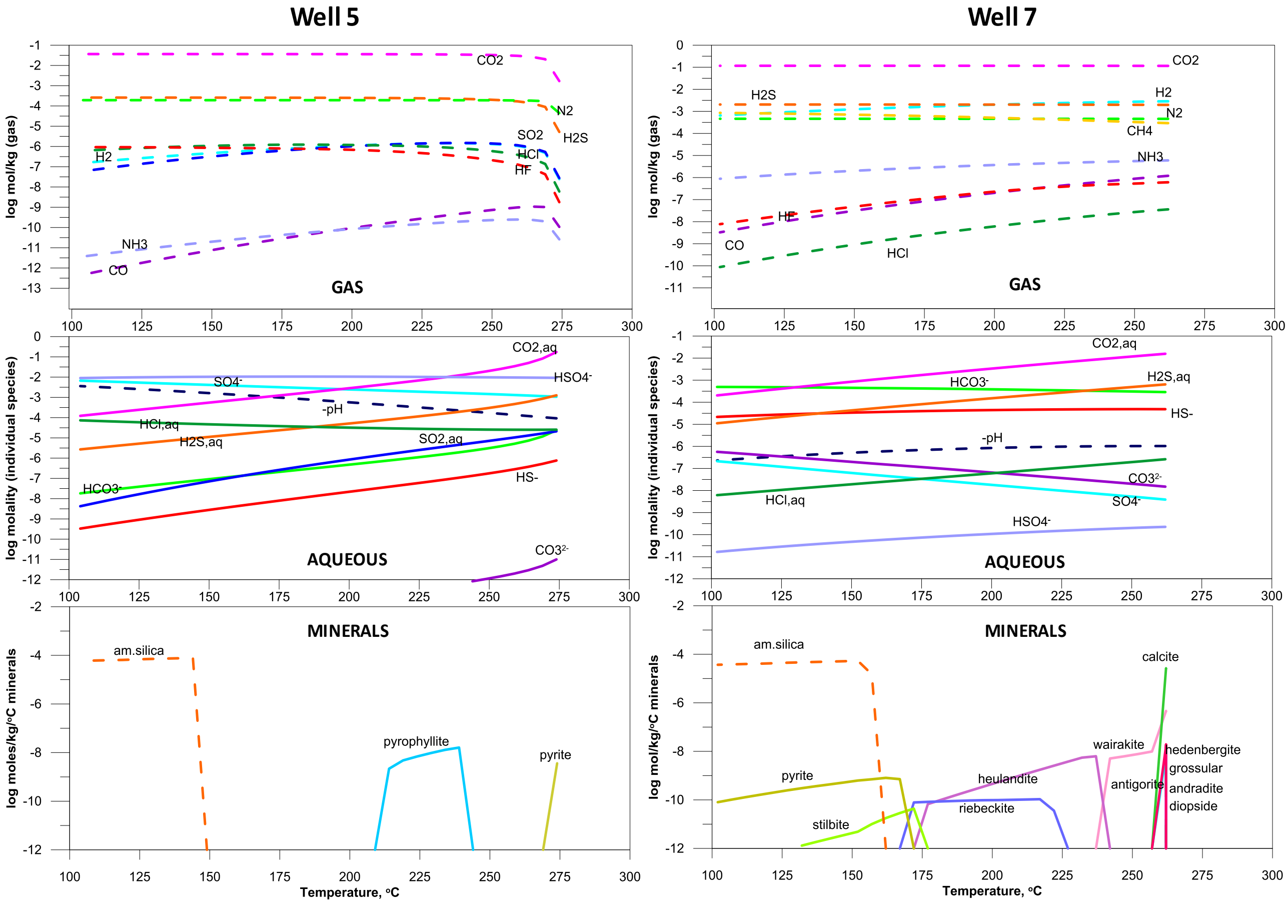

Figure 2: Boiling simulation of fluid from an acidic well (#5) and neutral well (#7). The Y-axis units for the mineral graphs are log moles/kg (of initial water) per °C. The "per degree C" arises because the minerals were fractionated as the boiling progressed, so that amount plotted is rate of precipitation per degree of temperature decrease.

3. WALL ROCK AND CASING REACTIONS

Geothermal fluids equilibrate with wall rocks as shown by studies of mineral saturation characteristics from many systems e.g., Reed and Spycher (1984); Giggenbach (1988); Pang and Reed (1998). The equilibration with wall rocks does not mean that fluids reach overall equilibrium with the primary minerals in the host rocks, because the wall rock minerals are commonly unstable in the presence of water at temperatures of a typical geothermal system. Rather, equilibration with wall rocks refers to a progressive process of reaction of the un-reacted initial fluid with initially fresh wall rock yielding a series of alteration mineral assemblages. This process is examined by incremental titration of a fresh andesite into a primary acidic fluid and a calculation of the equilibrium fluid and mineral composition at each increment from an infinite water/rock ratio to a small water/rock ratio. The chemical composition, oxidation state and pH of geothermal fluids are fixed by the reaction of waters with wall rocks as demonstrated by Reed (1992).

To determine where the excess iron in the Mt. Labo discharge originated, the host andesite was reacted with an estimated primary acidic fluid (Liquid A), and compared that result with the same fluid reacted with the well casing as outlined in Figure 3. The calculated iron concentrations, alteration minerals, and corrosion products are then compared to the actual alteration minerals in the drilled cuttings and corrosion products obtained at depth.

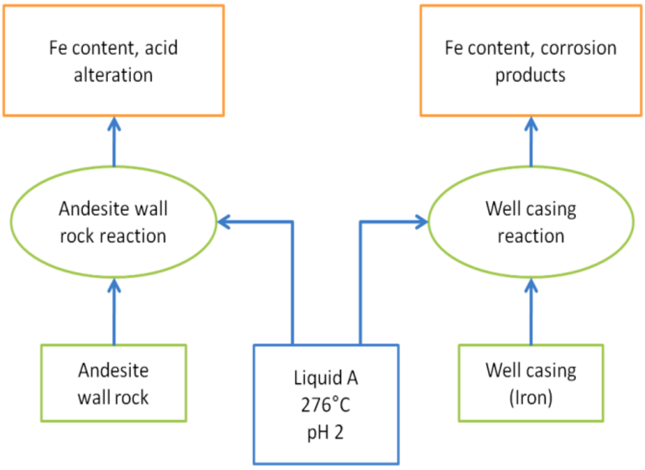

Figure 3: Schematic diagram of the wall rock and the well casing reactions of the parent fluid (Liquid A) at reservoir conditions

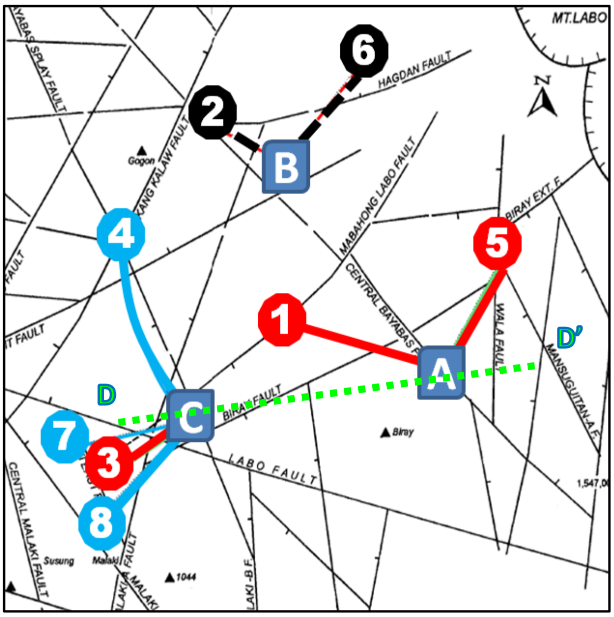

Figure 4: Wells in Mt. Labo. A and C mark the drilling pads identified in Figure 5 and discussed in the text. Wells #5 and #7 are the focus of this study. Line DD' transect is shown in Figure 5

3.1 Modeling of Liquid A

To examine whether the excess iron in Well #5 mostly came from the casing or the rock, Liquid A is modeled from a modification of Well #5 fluids. Since Well #5 contains an excess of iron as calculated in the boiling runs, directly using the actual concentration of Well #5 in the model will not reflect the condition of the unreacted reservoir fluids.

To correct this problem, the composition of the unreacted fluid referred to as Liquid A was estimated by modifying the actual concentration of Well #5, which intersects the postulated upflow of the system and taps the acidic fluids of the reservoir. Using Well #5 the initial concentration of the metals Fe^{2+}, Ni^{2+}, Zn^{2+} and Mn^{2+} were set to low values (magnitudes of 1.0 E-22m) and H_2SO_4 was added into the fluid to reach a starting pH of 2. An initial pH of 2 is a likely minimum for geothermal temperatures between 200 and 400°C indicated by alteration minerals in magmatic-hydrothermal systems as discussed by Reed (2013). This modified fluid, “Liquid A”, is used as the starting water composition for the calculations of the different geochemical processes shown in Figure 3.

3.2 Liquid A reaction with Andesite Host Rock

In the simulation of andesite wall rock reaction with Liquid A, the equilibration of the fluid with the andesite host rock is investigated by titrating andesite into the liquid-gas mixture at 276°C. It was assumed that the gas and liquid co-exist and simultaneously react with the host rocks. The mineral composition and equilibrium fluid derived from the calculations (Figure 6) are then compared to the actual alteration minerals found in the drill cuttings of the wells to check whether the actual alteration minerals match with the calculated minerals. From the reasonably matching results, the possible pH and composition of the fluids that were tapped by Well #5 were determined.

The actual acid alterations intersected by the wells of Pads A and C (Figure 5) indicate that alunite, pyrophyllite, and diaspore are common acid alteration minerals observed in shallow and deep sections intersected by the wells in Pad A (Well #5 location). Minimal acidic alteration was observed in Pad C (Well #7) and only at shallow depth.

The results of the water-rock reaction show that the reservoir pH increases as andesite reacts. The water-rock ratio of the actual state of the reservoir, before it reacted with the casing, was approximated by comparing the acid alterations that was formed in the model to the actual acid alterations from the drilling cuttings. The shaded blue region of Figure 6 shows the approximated region where likely the fluids tapped in Well #5 are in equilibrium with the alteration minerals at temperatures greater than 270°C and a pH range of 3 to 4. The calculated acid alteration minerals in this region, alunite and pyrophyllite match the actual observed acid alteration (alunite, diaspore, and pyrophyllite) from petrologic analyses by Ramos (1994) of drill cuttings obtained at the bottom of the wells where the temperature is at 276 °C. Other calculated alteration minerals such as quartz, anhydrite, chlorite and pyrite also match the actual alteration minerals in the well. In addition, in the region where the pH is 3 to 4, the iron concentration spikes at 33 to 36 ppm (log m (Fe, total) = -3), Figure 6. Beyond the spike, the aqueous iron concentration declines as more andesite reacts and the acidic fluid becomes neutralized.

3.3 Liquid A reaction with Well Casing

The same fluid is reacted with pure iron to simulate the reaction of Liquid A with the well casing for comparison of results with the scenario discussed is section 3.2. The iron is incrementally titrated into the liquid-gas mixture and the corresponding equilibrium concentration of iron complexes and the minerals at each increment are plotted in Figure 7. The pH of Liquid A increases as iron is consumed and the predominant iron complex that formed is $FeCl^+$ (equilibrium 7, Figure 7). The high chloride content of the brine drives the reaction to the right and transports the Fe^{2+} in the discharge resulting in a high Fe^{2+} level (157ppm). The amount of iron sulfides (pyrite) and iron oxides (hematite) formed in the process (Figure 7) were calculated, which is consistent with the composition of the blockage that was removed from the bottom of the Well #5, consisting of drilling mud and corrosion products namely, iron oxides (magnetite and hematite) and iron sulfides (mackinawite). These minerals were possibly deposited through the reaction of the steel casing of the well with corrosive acid fluids (Ramos and Delfin, 1997).

$$Fe^{2+}_{aq} + Cl^{-}_{aq} \leftrightarrow FeCl^{+}_{aq} \qquad (7)$$

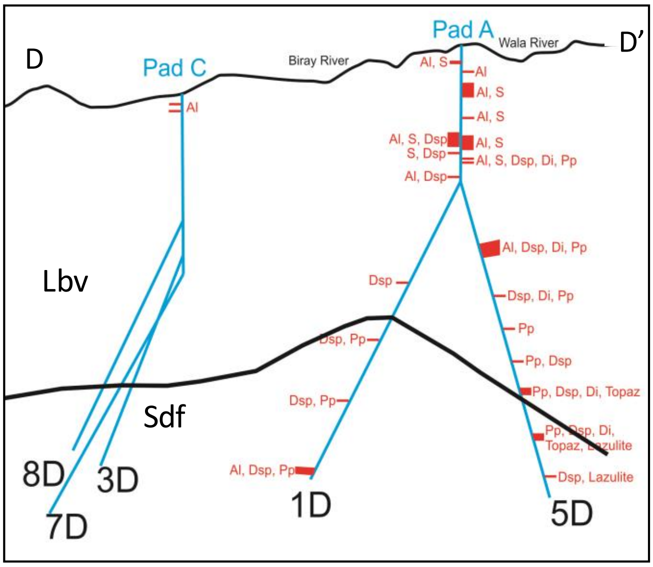

Figure 5: Acid alteration minerals of wells in Pad A (including Well #5) and Pad C (including Well #7) adapted from Panem (1998). The following abbreviations are used: Al – Alunite, Pp – Pyrophyllite, Dsp – Diaspore, S – Sulfur, Di – Dickite, Lbv - Labo Volcanics, Sdf - Susung Dalaga Formation. Alunite is found only at shallow depths in Pad C wells, probably of surficial origin. Pad A wells intersected many intervals containing acid alteration mineral down to lower depths, as is characteristic of alteration by magmatic sulfuric acid. Quartz, anhydrite, chlorite and pyrite (not shown) were also intersected at many depth intervals in both Pads A and C.

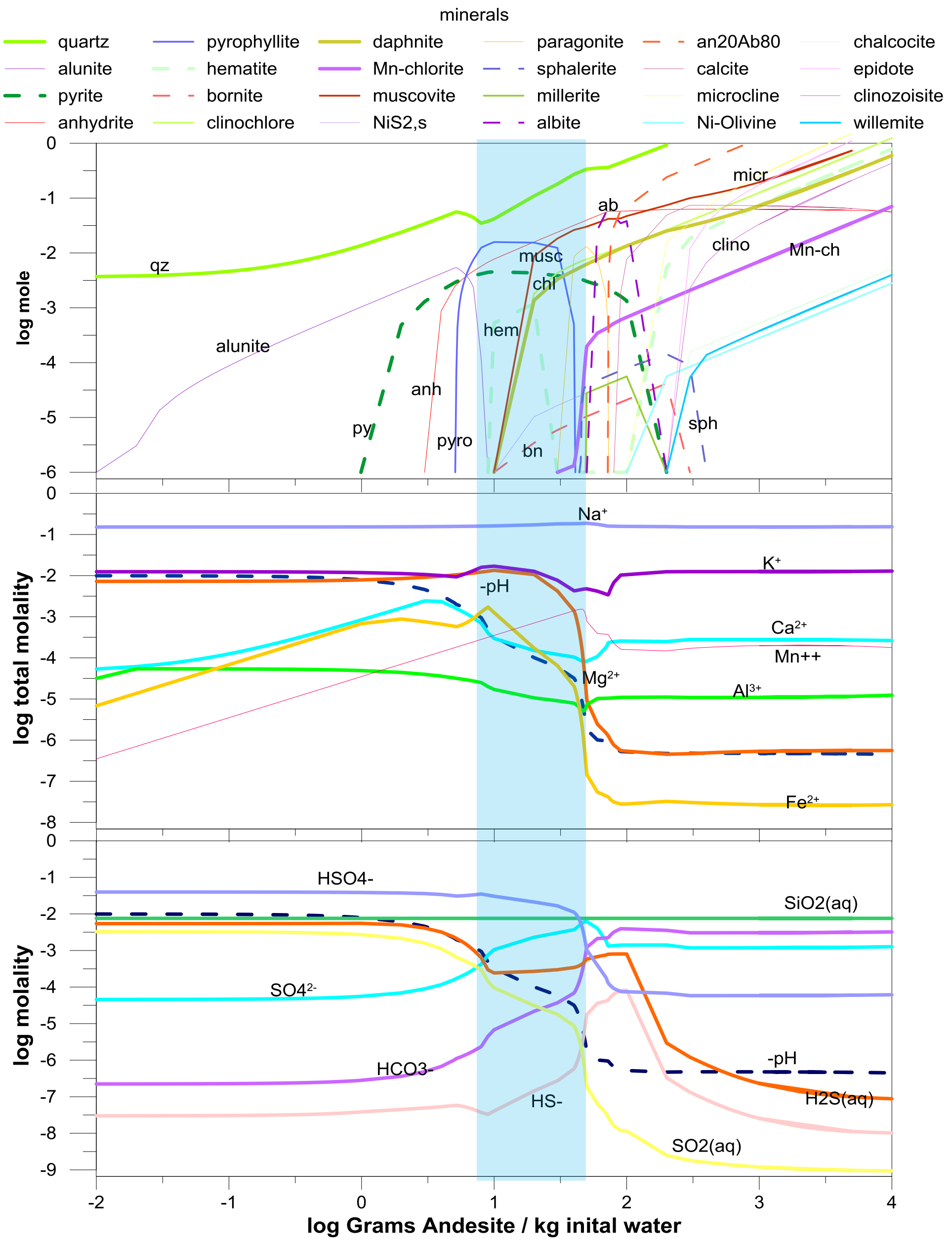

Figure 6: Reaction of Liquid A with fresh andesite at 276°C. The x-axis is in log grams of andesite titrated into a kilogram of the initial fluid (Liquid A).

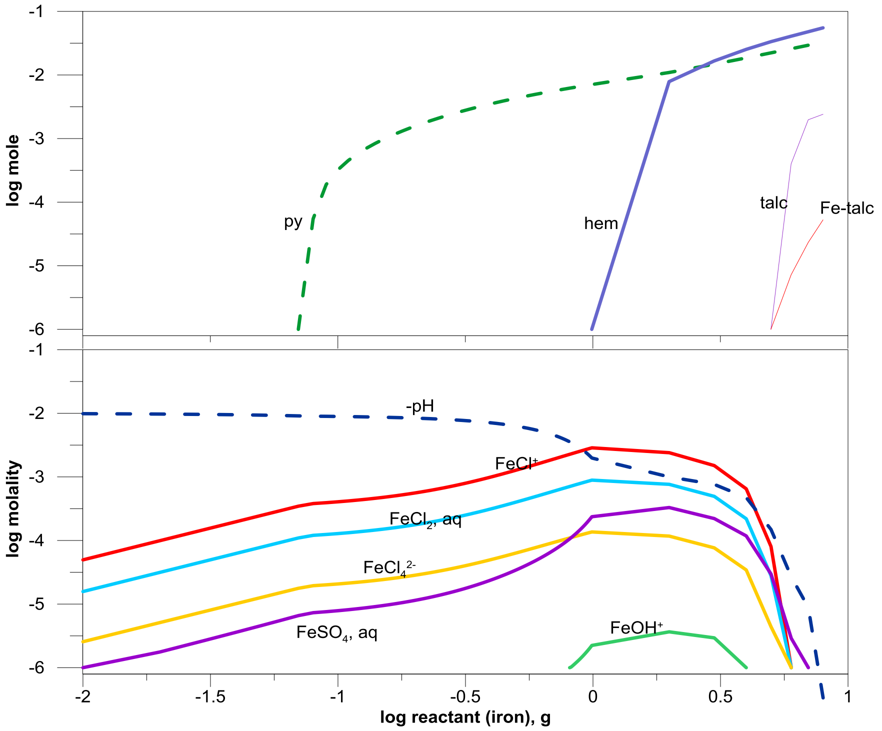

Figure 7: Liquid A reaction with steel casing at temperature of 267 ° C, corresponding to conditions at the bottom of Well #5

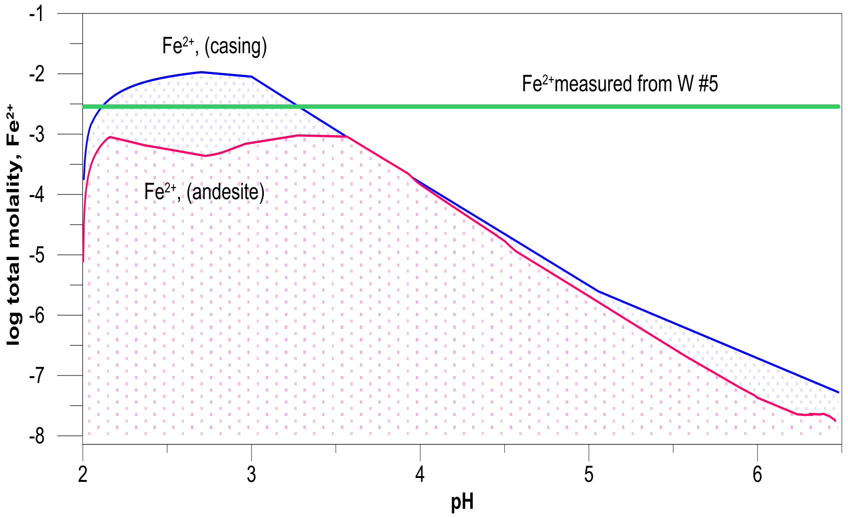

Figure 8: Comparison of total Fe concentration; blue line: calculated reaction concentration with steel casing; pink line: calculated reaction concentration with andesite; green solid line: measured iron concentration in Well #5 fluids.

3.4. The iron story

The total molality of Fe^{2+}calculated in the andesite and casing reactions (above) are plotted against pH in Figure 8, along with the actual measured iron concentration in Well #5. The highest iron concentration from the andesite reaction (log m (Fe, total) = -3 ~ 33-36 ppm) is one order of magnitude lower than the concentration from casing reaction (log m (Fe, total) = -2, ~ 370-390 ppm) and significantly lower than the discharge of the iron from Well #5 (log m (Fe, total) = -2.4, ~157 ppm). The highest Fe^{2+} concentration from andesite and casing reactions occurs at a pH<3.5. It is evident from this comparison that the Fe^{2+} measured in Well #5 did not solely come from the andesite host rock but some from casing corrosion, a conclusion supported by the finding of iron oxide and sulfide corrosion products in the blockage of the well.

4. CONCLUSION

Results of the water-rock reaction show that the fluid pH increases as rock (and iron) is consumed. The water-rock ratio of the actual state of the reservoir, before it reacted with the casing, was approximated by comparing the acid alteration minerals formed in the model to the actual mineral from the drilling cuttings. The computed alteration minerals from the model such as alunite pyrophyllite, quartz, pyrite, anhydrite and chlorite match the observed alteration (alunite, diaspore, pyrophyllite, quartz, anhydrite, chlorite, and pyrite) from petrologic analyses of drill cuttings from the bottom of the wells. The modeling result suggests that the most acidic reservoir fluids were pH<3.5 at 276°C, at which conditions the acid alteration minerals were in equilibrium with the acidic reservoir fluids and the high iron concentration in the well discharge originated largely from casing corrosion. In conclusion, the acidity is deep-seated in the postulated upflow fluids. The system may be neutralized when water-rock interaction takes place as the fluid are exposed to rock as it flows up and outward, such as towards the outflow region of the system.

ACKNOWLEDGEMENTS

The authors thank Energy Development Corporation (EDC) for support and permission that made this study possible. The authors also thank Dr. James Palandri for assistance with computing and acknowledge support from US NSF grant EAR0507181 for thermochemical data base development.

REFERENCES

Aurelio, M.A.: Tectonics of the Philippines revisited. *Journal of the Geological Society of the Philippines,* **55** (2000) 119-183.

Delfin, M.C.Z., et al.: Mt. Labo Geothermal Project Resource Assessment Update (Draft Report), *PNOC-EDC Internal Report* (1995).

Delfin, F.G.: Deep Geothermal Resource in the Philippines: An Update of two PNOC EDC Exploration *Projects*, *Japan International Geothermal Symposium,* (1997)

Giggenbach, W.: Geothermal Solute Equilibria. Derivation of Na-K-Mg-Ca geoindicators, *Geochemica et Cosmochimica Acta,* **52**, (1998) 2749-2763.

Japan International Cooperation Agency (JICA) Metal Mining Agency of Japan: Report on regional survey for mineral resource in the Bicol area, Republic of the Philippines, (1999)

Maturgo, O.O., et al.: Characteristics of the Volcanic-Hydrothermal System in Mt. Labo, Philippine: Implications to Development, *Proceedings World Geothermal Congress,* Japan (2000).

Pang, Z.H., and Reed. M.H.: Theoretical Chemical Thermometry on Geothermal Waters: Problems and methods, *Geochemica et Cosmochimica Acta,* **62** , (1998) 1083-1091.

Panem. C.C.: Correlation of Subsurface Structures, Permeability and Acid Zones in Mt. Labo Wells, *PNOC-EDC Internal Report* (1998).

Ramos, S.G.: Petro Analysis of LB-5D, PNOC-EDC *radio message* (1994).

Ramos, S.G. and Delfin, M.C.Z.: Petrologic Evaluation of Well LB5D Blockage, *PNOC-EDC Internal Report* (1997).

Reed, M.H.: Computer Modeling of Chemical Processes in Geothermal Systems: Examples of Boiling, Mixing and Water-Rock Reaction, *Guidebook,* UNITAR/UNDP Center on Small Resources, New York USA (1992).

Reed, M.H.: Calculation of Simultaneous Chemical Equilibria in Aqueous-Mineral-Gas Systems and its Applications to Modeling Hydrothermal Processes, *Reviews in Economic Geology,* **10,** (1998), 109-124.

Reed, M.H., and Spycher, N.: Calculation of pH and Mineral Equilibria in Hydrothermal Waters with Application to Geothermometry and Studies of Boiling and Dilution, *Geochemica et Cosmochimica Acta,* **48** (1984), 1479-1492.

Reed, M.H., et.al: SOLVEQ-XPT: A Computer Program for Computing Aqueous-Mineral-Gas Equilibria, *User's Manual,* Department of Geological Sciences University of Oregon, Eugene OR (2010)

Reed, M.H., et.al: CHIM-XPT: A Program for Computing Reaction Processes in Aqueous-Mineral-Gas and MINTAB Guide, *User's Manual,* Department of Geological Sciences University of Oregon, Eugene OR (2010)

Reed, M.H., et.al: The Butte Magmatic-Hydrothermal System: One Fluid Yields All Alteration and Veins, *Economic Geology,* **108** (2013)

Symonds, R.B., et.al: Magmatic gas scrubbing: implications for volcano monitoring, *Journal of Volcanology and Geothermal Research,* **108**, (2001) 303-341.